FRACTAL DIMENSION OF THE TRAJECTORY OF A SINGLE PARTICLE DIFFUSING IN CROWDED MEDIA

LAURA PITULICE [1,2], DANA CRACIUN [3], EUDALD VILASECA [4], SERGIO MADURGA [4], ISABEL PASTOR [4], FRANCESC MAS [4], ADRIANA ISVORAN [1]

[1]*Departament of Biology-Chemistry, West University of Timisoara, Str. Parvan Nr.4, 300223 Timisoara (Romania), E-mail: ldpitulice@gmail.com E-mail: aisvoran@yahoo.com*
[2]*University „Al.I.Cuza", Str. Carol I nr.11 700506 Iasi, (Romania) - temporary affiliation, E-mail: ldpitulice@gmail.com*
[3] *Teacher Training Departament, West University of Timi□oara 4 V. Pârvan, Timi□oara, Romania, E-mail: craciundana@gmail.com*
[4]*Department of Physical Chemistry and the Research Institute of Theoretical and Computational Chemistry (IQTCUB) of the University of Barcelona (UB), C / Martí i Franquès, 1, 08028 Barcelona (Spain), E-mail: eudald.vilaseca@ub.edu E-mail: s.madurga@ub.edu E-mail:i.pastordelcampo@gmail.com E-mail: fmas@ub.edu*

Abstract. Using Monte Carlo simulations we have modeled the diffusion of a single particle in two- and three-dimensional lattices with different crowding conditions given by distinct obstacles size and density. All registered data emphasize that diffusion process is anomalous and diffusing particle describes fractal trajectories. We have introduced a new time-scale fractal dimension, d_m, which is related to the anomalous diffusion exponent, α. This allows us to relate the well-known length-scale fractal dimension of the random walk, d_w, to the new one introduced here as a time-scale fractal dimension. Moreover, the 3D simulations consider similar conditions to those used in our previous FRAP experiments in order to reveal the relationship between the length and time-scale fractal dimensions.

Key words: diffusion, random walk, crowded media, fractal dimension, long-range correlation.

1. INTRODUCTION

Diffusion is one of the most important transport phenomena that occur in living organisms. The living cell has been described as inhomogeneous, disordered and crowded media [1] and diffusion process in such environment is considered anomalous [2, 3]. Considerable theoretical and experimental work concerning diffusion in living organisms has been performed, we only emphasis that earlier studies were excellently reviewed by Havlin and Ben-Avraham [3] and Dix and Verkman [4] and more recent ones by Saxton [5]. Most of the theoretical studies revealed that in crowded environment diffusion is anomalous, but experimental studies revealed both anomalous [6, 7] and normal diffusion [8] in crowded systems, depending on the time scale of the experimental method. It means that the hypothesis that crowding causes anomalous diffusion is still controversial and much understanding could be offered by theoretical models resulting from simulation works.

The study aims at analyzing the trajectory characteristics of a single particle diffusing in both two- (2D) and three-dimensional (3D) crowded media and correlates them with the parameters determining anomalous diffusion in such systems. In particular, we introduce a new time-scale fractal dimension, d_m, related with the well-known length-scale fractal dimension, d_w. The effect of obstacles size and density is tested. Based on the findings, we further compare the time-scale fractal dimensions of the trajectory obtained from both 3D simulations and FRAP experiments [9]. The experimental data are used to infer the fractal dimension of the particle trajectory based on the model tested in 2D diffusion.

2. METHOD

2.1 Anomalous diffusion and fractal dimensions

A diffusion process taken by a solute in dilute solutions can be described with the well-known Einstein-Smoluchowski equation for Brownian motion:

$$\left\langle r^2(t)\right\rangle = (2d)Dt \tag{1}$$

where d is the topological dimension of the medium where the process is embedded and D is its diffusion coefficient [10-12]. In crowded media, typically in vivo and in a great number of in vitro experiments, the existence of different macromolecular species hinders the diffusion process. In these cases, Eq. (1) must be generalized to a more complex process, known as anomalous diffusion [6, 11-13] which can be described by:

$$\left\langle r^2(t)\right\rangle = (2d)\Gamma t^{\alpha} \tag{2}$$

where α is defined as the anomalous exponent ($0 < \alpha < 1$ is the case of subdiffusion and $\alpha > 1$ holds for the case of superdiffusion) and Γ is a generalized transport coefficient, also known as anomalous diffusion coefficient, of units (length^2/time$^{\alpha}$), its value depending on the medium crowding degree.

The motion of single particle can be described using the concept of random walk [14] because the particle movement consists of a succession of random steps. The trajectory of a random walk is obtained by connecting the visited sites and it has interesting geometric properties described in terms of fractal geometry [15]. Also, the fractal geometry proved to be useful to explain features of diffusion in crowded media [16]. The random walk motion is quantitatively described by fractal dimension of the random walk (d_w) that is related to the anomalous diffusion exponent through the following relationship [10]:

$$d_w = \frac{2}{\alpha} \tag{3}$$

where $d_w = 2$ for normal diffusion and $d_w > 2$ for anomalous diffusion. Instead of determining the fractal dimension of the random walk trajectory using the well-known box-counting algorithm, we have introduced an algorithm similar to that used to compute the fractal dimension of the protein backbone [17]. The novelty of the approach, as far as we know, is two-fold: first, the algorithm is applied on particle diffusion and second, it is based on the temporal sequence of the trajectory.

Let L_m be the length of the trajectory for different step intervals, m, calculated according to the following equation:

$$L_m = \sum_{i=1}^{\mathrm{int}(T/m)} \left(\sqrt{(x_{i+m} - x_i)^2 + (y_{i+m} - y_i)^2 + (z_{i+m} - z_i)^2} \right) \quad (4)$$

where x_i, y_i, z_i are the spatial coordinates of diffusing particle at step i and T represents the total number of time steps. The dependence of L_m on the time-scale m will be given by:

$$L_m \sim m^{(1-d_m)} \quad (5)$$

as usual in length-scale fractal dimension calculations, where d_m is a new fractal dimension on this time-scale.

In order to relate the two fractal dimensions, d_w in length-scale and d_m in time-scale, we correlate the time-length of the trajectory, L_m, with the root mean square displacement, $\langle r_m^2 \rangle$, taking into account that this root mean square displacement is computed as the mean of different lengths of the trajectories "walked" by the particle in a time step interval, m. It can be seen that

$$L_m = \sqrt{\langle \mathrm{r}_\mathrm{m}^2 \rangle} \frac{T}{m} \quad (6)$$

On the one hand, $\langle r_m^2 \rangle$ must follow the same time-scale on the general diffusion relation, Eq. (2). Then,

$$\langle \mathrm{r}_\mathrm{m}^2 \rangle \sim m^{\alpha} \quad (7)$$

and relating the two time-scale parameters L_m (Eq. (5)) and $\langle r_m^2 \rangle$ (Eq. (7)) we get the following equation:

$$L_m \sim m^{\frac{\alpha}{2}-1} \quad (8)$$

Then, from both power laws Eqs. (5) and (8) we obtain the relation between the two scale exponents (Eq. (9)) and also between the two fractal dimensions (Eq. (10)):

$$d_m = 2 - \frac{\alpha}{2} \quad (9)$$

$$d_w = \frac{1}{2 - d_m} \quad (10)$$

It is important to note that the new time-scale fractal dimension, d_m, presents similarities to the fractal dimension of the protein backbone, d_f, computed from the *log-log* plots of the backbone length with number of residues that yield the $(1/d_f\text{-}1)$ slope [17]. The fractal dimension of the protein backbone has two different values corresponding to the local or global scaling regime, depending on the considered number of residues. Similarly, the computed d_m is associated to a local scaling regime, due to different particle trajectory lengths calculated for the same time interval, especially for small m values.

Moreover, $d_m = 2\text{-}\alpha/2$, as given by Eq. (9), reaches its lowest value, $d_m = 3/2$, for cases of normal diffusion, $\alpha = 1$, being consistent with the length of the trajectory, L_m, given by Eq. (6), using the Eq. (1),

$$L_m = \sqrt{(2d)Dm}\,\frac{T}{m} \sim \mathrm{m}^{-1/2} \tag{11}$$

and also with the scaling exponent, (1-d_m) = -0.5 from Eq. (5). For anomalous diffusion, $\alpha < 1$ and $d_m > 3/2$. This is also consistent with the value of $d_w > 2$ for obstructed diffusion that gives the anomalous exponents.

2.2 Simulation model

The random walk simulations were performed using custom-written Fortran 77 programs. Regarding the 2D computations, the particle diffusion was simulated inside a square lattice of 50 sites edge length, with cyclic boundary conditions. The particle occupies 1 site in the lattice and the immobile obstacles are randomly distributed considering different site density occupancy, up to the percolation threshold: 0, 0.1, 0.2, 0.3 and 0.4 respectively. The obstacles have square shape. Different sizes of the obstacles are considered according to edge length chosen: 1, 3, 5, and 7 sites, respectively. A random number is generated to choose one of the four nearest neighbor sites of the single-particle to move. The particle moves only if the selected position is empty. Each simulation has 10.000 time steps and every run was repeated 500 times with a different initial particle disposition. For each simulation the trajectory length and the mean squared displacements are averaged along these repetitions.

The computational model of the particle diffusion in 3D obstructed media was tailored in an analogous way with the features of our previously performed FRAP experiments to allow the proposed comparison. The model considers a one site particle diffusing in an 80x80x80 cubic lattice with cyclic boundary conditions in which obstacles are randomly distributed. The tracer-obstacles size ratio is similar with that of the protein-crowding agent used during experimentation. Thus, two different obstacle dimensions are set: 27 sites corresponding to a 3x3x3 sites cube, and 179 sites according to a 7x7x7 sites cube with removed edge and vertex sites, to reach a quasi-spherical shape. The obstacles are mobile to simulate the motion of the experimental crowding agent. The mobility is controlled by a probability factor related to the obstacles size (0.75 for the small ones and 0.1 for the big ones). The density of sites occupied by obstacles is further referred to as the excluded volume determined by their presence (Φ). The excluded volume values are: 0.031, 0.062, 0.124 and 0.187 according to our experimental data. The subsequent simulation steps are already explained in detail elsewhere [9, 18]. Both 2D and 3D simulation data are then used to compute the following parameters: the anomalous diffusion exponent, α, from the slope, α-1, of the $\log(< r^2 > / t)$ *versus* $\log(t)$ plot and subsequently the fractal dimension of the random walk, d_w, according to Eq. (3); the fractal dimension of the random walk trajectory, d_m, from the slope, 1-d_m, of the $\log(L_m)$ *versus* $\log(m)$ plot. The calculated coefficients are then used to correlate the fractal aspects of the trajectory with the anomalous diffusion of the single particle random walk in a crowded environment. Moreover, we try to quantitatively characterize the dependence of diffusion process on the size and density of randomly distributed obstacles.

2.3 FRAP experiments

FRAP experimental technique is able to study the properties of a tracer particle (e.g. protein) in a solution containing high concentration of other macromolecules. Therefore, the experimental results of a previous work, based on this particular technique [7], are used to make the comparison with our 3D computational data [9]. The experiments investigated the FITC-alpha-chymotrypsin complex diffusing in an aqueous buffer in which two different types of Dextran was dissolved as crowding agent (Dextran with Mw = 48.6 kDa (denoted as D1) and Dextran with Mw = 409.8 kDa (denoted as D2)). Dextran was chosen as a crowding agent because it can readily be represented in computer simulations as repulsive hard spheres of the appropriate size. D1 corresponds to the small obstacles (3x3x3) and D2 to the big obstacles (7x7x7R) considered in our 3D simulations. The Dextran concentration in samples was up to 300 mg/mL, and thus the excluded volume (from 0 to 0.2) was similar with that considered in the Monte Carlo simulations. FRAP data were fitted with a versatile expression for subdiffusion in bulk solution [7] from which the α parameter values were obtained (see Table 3). The experiments further details have been explained elsewhere [9].

3. RESULTS AND DISCUSSIONS

3.1 2D Monte Carlo simulation

In all the studied cases, the obtained $\log\left(< r^2 > / t\right)$ *versus* $\log(t)$ diagrams for the single particle diffusion in lattices with obstacles have features corresponding to anomalous diffusion in good correlation with those presented in specific literature [3 - 6, 9]. We illustrate such plots in Fig. 1 for the single particle diffusion in a 2D obstructed lattice with square obstacles with the same excluded volume (Φ = 0.3) and distinct sizes: 1x1, 3x3, 5x5 and 7x7, respectively. For comparison, Fig. 1 also presents the $\log\left(< r^2 > / t\right)$ *versus* $\log(t)$ plot for diffusion in a 2D unobstructed lattice (continuous line). Figure 1 reveals classical diffusion for single particle movement in unobstructed lattice and anomalous diffusion for obstructed lattices. There is a clear distinction between the allure of the plot for obstacles having different sizes: the slope of the decreasing regions of curves being smaller for bigger obstacles. It means that anomalous diffusion exponent, α, decreases with increasing size of obstacles (these exponents are presented in Table 1) reflecting the higher complexity of the environment obtained when small obstacles are distributed in the same density as bigger ones.

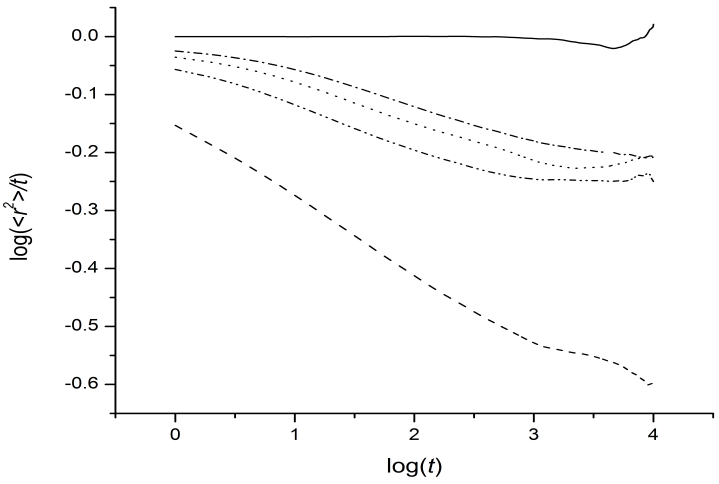

Figure 1 - The $\log(< r^2 > / t)$ versus $\log(t)$ plots at constant obstacles density (0.3) with different sizes: 1x1 (dash line), 3x3 (dash-dot-dot line), 5x5 (dot line) and 7x7 (dash-dot line). The $\log(< r^2 > / t)$ versus $\log(t)$ plot (continuous line) in the absence of obstacles.

Table 1
The values of the anomalous diffusion exponent α, trajectory fractal dimension of the, d_m, and random walk exponent for single particle movement in 2D lattices with distinct fixed obstacle density and sizes. The estimated errors of the parameters are below 1%.

Obstacle size	Φ	α	$d_w=2/\alpha$	d_m	$d_w=1/(2-d_m)$
No. Obs.	0	1.000	2.000	1.507	2.027
1x1	0.1	0.966	2.070	1.513	2.053
	0.2	0.927	2.158	1.530	2.126
	0.3	0.863	2.317	1.565	2.299
	0.4	0.731	2.735	1.630	2.702
3x3	0.1	0.979	2.043	1.515	2.062
	0.2	0.953	2.099	1.525	2.107
	0.3	0.929	2.153	1.539	2.169
	0.4	0.890	2.247	1.558	2.264
5x5	0.1	0.980	2.040	1.516	2.067
	0.2	0.960	2.083	1.527	2.115
	0.3	0.935	2.138	1.539	2.169
	0.4	0.903	2.215	1.554	2.242
7x7	0.1	0.980	2.041	1.517	2.068
	0.2	0.960	2.084	1.527	2.114
	0.3	0.935	2.140	1.539	2.171
	0.4	0.906	2.209	1.553	2.239

Table 1 also shows the values of the fractal dimension of the random walk, d_w, calculated with Eq. (3). As anomalous diffusion is considered to arise partly as a result of the fractal nature of the particle trajectories [19] we have also investigate the fractal dimension of the trajectory of a single particle movement. The results are presented in Table 1. Figure 2 illustrates the time-scale computation of the fractal dimension of the trajectory, dm, from the slope of $\log(L_m)$ *versus* $\log(m)$ plot for the case with an obstacle excluded volume of Φ=0.3.

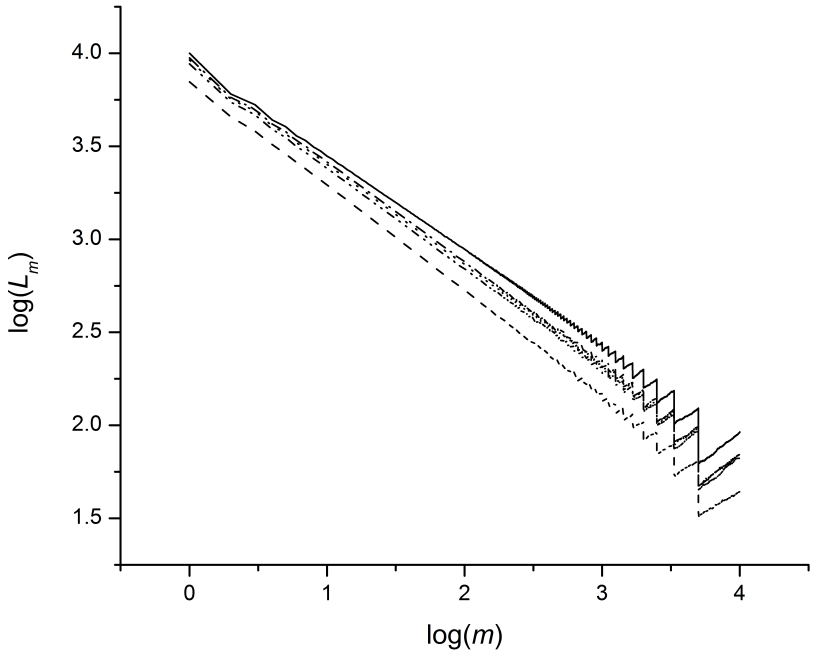

Figure 2 - Double-logarithmical plot of the trajectory length in 2D media versus step interval without and with obstacles of different sizes at 0.3 concentration: 1x1 (dash line), 3x3 (dash-dot-dot line), 5x5 (dot line) and 7x7 (dash-dot line)

Finally, we can observe from Table 1 that the d_w values, obtained both using the Eqs. (3) and (10), are similar. It can be observed that for each particular spatial distribution of the occupied sites the values of the anomalous diffusion exponent, α, the fractal dimension of random walk, d_w, and the time-scale fractal dimension, d_m, are rising with the increase of the obstacles concentration. For the same concentration of obstacles these values decrease with obstacle size. All these results are in good agreement with other published data [3, 4, 9, 20].

3.2 3D Monte Carlo simulation versus FRAP experiments

The findings of the previous section have encouraged us to investigate the application of Eq. (9) on 3D cases both by simulation and experimentation. To obtain comparable results, the 3D simulations considered mobile obstacles similarly with the experimental conditions (Table 2).

Table 2
The values of the anomalous diffusion exponent α, trajectory fractal dimension, d_m, and random walk exponent, d_w, for single particle movement in 3D lattices with distinct mobile obstacle density and sizes. The parameters estimated errors are below 1%.

Obstacle size	Φ	α	$d_w=2/\alpha$	d_m	$d_w=1/(2-d_m)$
3x3x3	0.031	0.998	2.005	1.519	2.080
	0.062	0.996	2.009	1.520	2.084
	0.124	0.992	2.017	1.522	2.092
	0.187	0.987	2.026	1.523	2.098
7x7x7 R	0.031	0.997	2.007	1.512	2.048
	0.062	0.993	2.014	1.519	2.081
	0.124	0.986	2.028	1.520	2.084
	0.187	0.979	2.044	1.524	2.101

The previously performed FRAP experiments allowed us to obtain the α parameter values for the crowded systems under research. Instead, this experimental technique does not facilitate to record the diffusing particle trajectory. As a result, the d_m values have been indirectly retrieved based on the α values using the correlation given by Eqs. (10) and (3). Subsequently, the d_w values have been calculated using the d_m values. All data are found in Table 3. It is worth mentioning here that, the relationship proposed by Eq. (10) has been proved to be adequate when correlating the two manners of obtaining the d_w values.

Table 3
The values of the anomalous diffusion exponent α from FRAP experiments [9], and the corresponding obtained values of the trajectory fractal dimension, d_m, and random walk exponent, d_w. The estimated errors of the parameters are below 5%.

Dextran size	Φ	α	$d_w=2/\alpha$	d_m	$d_w=1/(2-d_m)$
D1 (48.6 kDa)	0.031	0.94	2.13	1.53	2.13
	0.062	0.88	2.30	1.56	2.30
	0.124	0.90	2.22	1.60	2.22
	0.187	0.87	2.30	1.60	2.29
D2 (409.8 kDa)	0.031	0.90	2.22	1.55	2.20
	0.062	0.82	2.44	1.59	2.44
	0.124	0.82	2.44	1.59	2.44

It can be observed from Table 3 that for each given size of the crowding agent, D1 (Dextran with Mw = 48.6 kDa) and D2 (Dextran with Mw = 409.8 kDa), the particle trajectory is more fractal as the Dextran concentration is higher. Obviously, the particle in its diffusion movement has to avoid many more obstacles following a more fractal path. Additionally, for the same occupied volume (same crowder density) the particle trajectory is more fractal as the crowder size is bigger. The explanation may come from the fact that smaller

obstacles have an increased mobility than bigger ones allowing the particle to diffuse more easily through the media. On the contrary, when fixed, these small obstacles rip the space obliging the diffusing particle to describe a more fractal trajectory. This is in accordance with our 2D simulations in which crowder particles were kept immobile.

Looking at α, d_m and d_w values obtained by 3D simulations (Table 2), one can see they present a very small variation from one case to another. The expected magnitude of the crowding effect is strongly dependent upon the relative sizes and concentration of the crowding species [21]. Within our 3D computations, low densities of obstacle were chosen according to the experimental approach and thus the behavior is likely to occur. On the other hand, there are no spatial constrains like in 2D media and no other aspects, such as interactions between diffusing particle and obstacles, are taken into account. Even though, the dm values have a variation with crowder concentration similar with that obtained by experimentation for each obstacle size. Opposite to the experimental data, for a certain obstacle density the particle exhibits a more fractal trajectory as crowder is smaller.

It has to be considered that models proposed both by simulation and experimentation have the advantage to be intuitive and focused on specific aspects of crowding. However, they do not comprise all details of a native-like cellular media. Therefore, if more realistic features are introduced when modeling such microenvironments it will lead to a better understanding of these complex systems.

4. CONCLUSIONS

Within this paper we have studied, on the one hand, the single particle movement in two dimensional obstructed square lattices using a Monte Carlo simulation algorithm. Two different aspects of the crowding effect on the fractality of diffusing particle trajectory have been analyzed: the effect of the obstacle concentration expressed in occupied sites and the effect of the spatial distribution of the occupied sites, expressed in different obstacle sizes. In all investigated cases, the particle trajectory was fractal and diffusion was registered as anomalous. The degree of fractality of the trajectory and consequently the density of explored sites and the anomalous diffusion rise along with the increase of obstacles density and decrease as the obstacles become bigger. These results confirm the hypothesis that anomalous diffusion is a consequence of the fractal nature of particle trajectory [20] as a higher fractal dimension of diffusing particle trajectory correspond to a more anomalous diffusion.

On the other hand, we have performed 3D simulations according to previously done FRAP experiments [9] in order to test the correlation between the length and time-scale parameters. The experimental data also demonstrate the correlation between the fractality of the particle trajectory and the size, concentration and mobility of the crowding agent. This is to say that a greater mobility of the a priori more obstructed obstacles yields a less fractal trajectory of the diffusing particle.

Also, our results confirm that anomalous diffusion is a result of a microscopic stochastic mechanism [22]. The deterministic nature of considered

crowded systems is expressed through the dependencies of single particle displacements on system parameters. These dynamical correlations are incorporated in a very complex way resulting in a fractal trajectory of diffusing particle.

All data presented here emphasis that for a better understanding of diffusion as a macroscopic transport one must take into account the microscopic dynamics of the system.

ACKNOWLEDGMENTS

For the first author, this work was financially supported by the Sectorial Operational Programme Human Resources Development 2007 – 2013 through the project *Transnational network for integrated management of postdoctoral research in the field of Science Communication. Institutional set up (postdoctoral school) and scholarship program (CommScie)*, POSDRU/89/1.5/S/63663.

REFERENCES

[1] A.B. Fulton, Cell **2** 345-347 (1982).
[2] S.B. Zimmerman, A.P. Minton, Annu. Rev. Biophys. Biomol. Struct**. 22**, 27-65 (1993).
[3] S. Havlin, D. Ben-Avraham, Adv. Phys. **51**, 187-292 (2002).
[4] J.A. Dix, A.S. Verkman, Annu. Rev. Biophys. **37**, 247-263 (2008.
[5] M.J. Saxton, Biophys. J. **103**, 2411-2422 (2012).
[6] D. S. Banks, C. Fradin, Biophys. J. **89**, 2960-2971 (2005).
[7] I. Pastor, E. Vilaseca, S. Madurga, J.L. Garces, M. Cascante, F. Mas, J. Phys. Chem. B. **114**, 4028-4034 (2010).
[8] A. Shakhov, R. Valiullin, J. K□rger, Phys. Chem. Lett. **3**, 1854-1857 (2012).
[9] E. Vilaseca, I. Pastor, A. Isvoran, S. Madurga, J.L. Garces, F. Mas, Theor. Chem. Acc. **128**, 795-805 (2011).
[10] D. Ben-Avraham, S. Havlin, *Diffusion and Reactions in Fractals and Disordered Systems*, Cambridge University Press, New York, USA, 2000.
[11] J.P. Bouchaud, A. Georges, Phys. Rep. **195**, 127-293 (1990).
[12] R. Metzler, J. Klafter, Phys. Rep. **339**, 1-77 (2000).
[13] T.J. Feder, I. Brust-Mascher, J.P. Slattery, B. Baird, W.W. Webb, Biophys J. **70**, 2767-2773 (1996).
[14] K. Pearson, Nature **72**, 294- 242 (1905).
[15] B.D. Hughes, *Random walks and random environments*, Oxford University Press, New York, USA, 1996.
[16] Y. Meroz, I. Eliazar, J. Klafter, J. Phys. A. **42**, 434012 (2009).
[17] G.T. Dewey, *Fractals in molecular biophysics*, Oxford University Press, New York, USA, 1997.
[18] E. Vilaseca, A. Isvoran, S. Madurga, I. Pastor, J.L. Garces, F. Mas, Phys. Chem. Chem. Phys. **13**, 7396-7407 (2011).
[19] A. R. Osborne, R. Caponio, Phys. Rev. Lett. **64**, 1733-1739 (1990).
[20] M. J. Saxton, Biophys. J. **64**, 1053-1062 (1993).
[21] H-X Zhou, G. Rivas, A.P. Minton, Annu. Rev. Biophys. **37**, 375-397 (2008).
[22] T. Geisel, J. Nierwetberg, Phys. Rev. A **29**, 2305-2390 (1984).